

Modelling the equatorial emission in a microquasar

T. Smponias

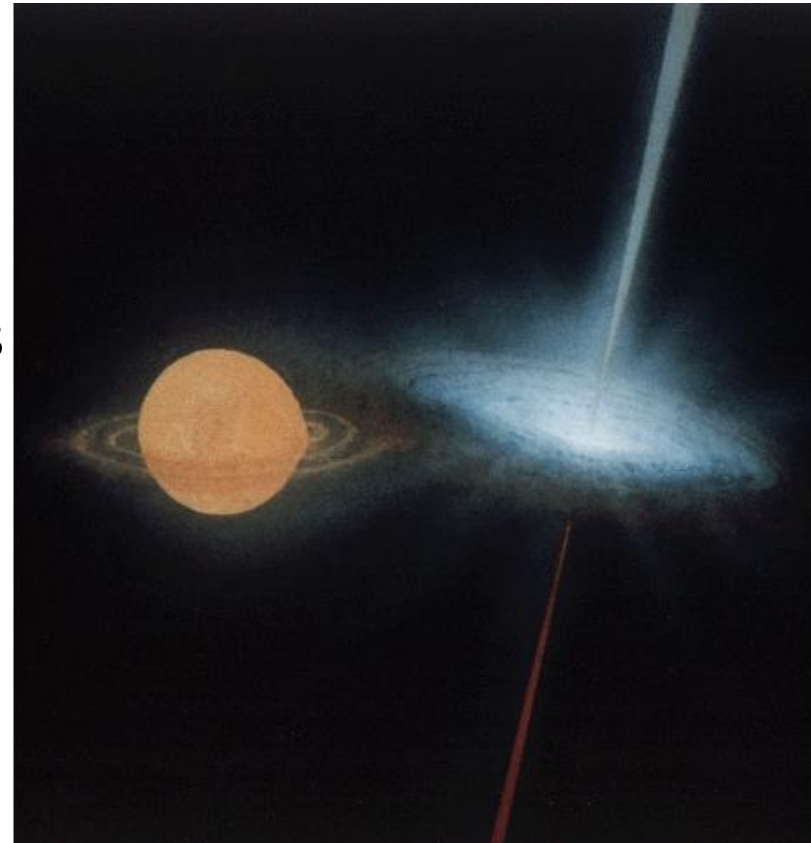
In collaboration with:

T. Kosmas (University of Ioannina)

The active environment of SS433

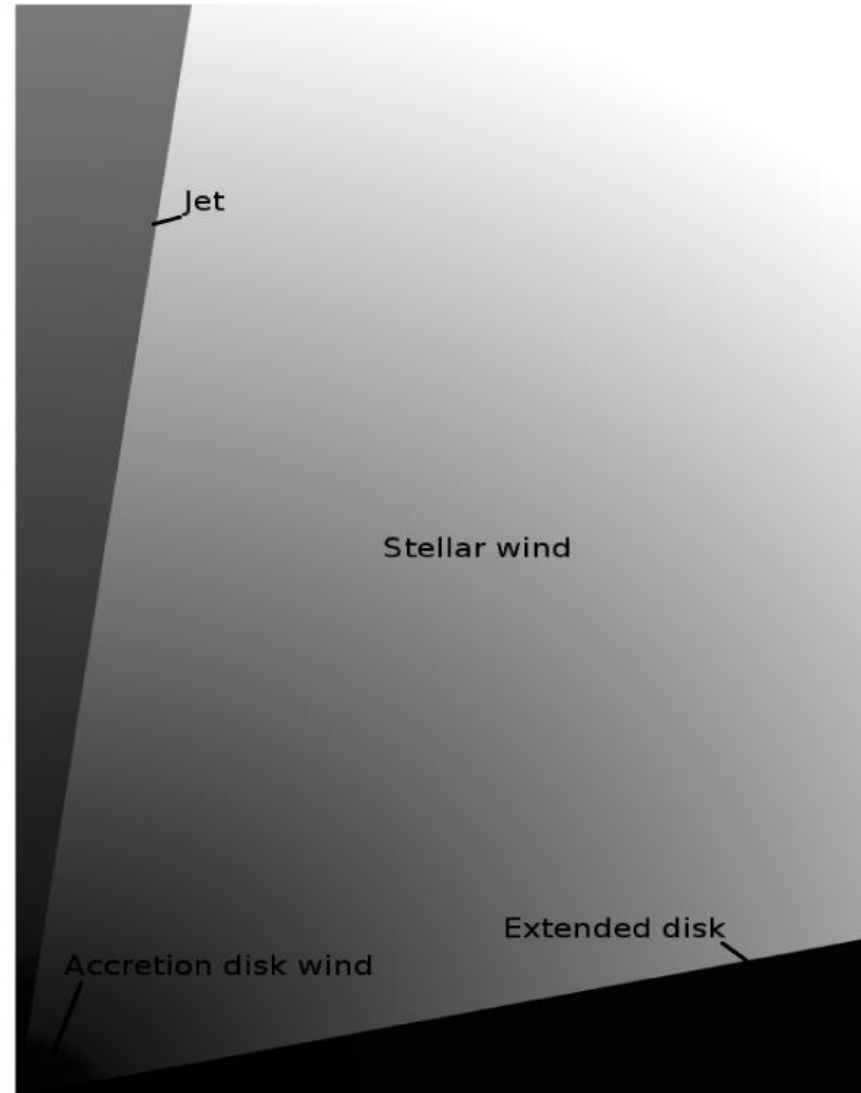
- Close binary system, including a collapsed stellar remnant and a late A-type star, with a stellar wind component
- Matter from the star accretes onto the collapsed object
- An outer circumbinary ring surrounds the whole system
- The jets are emitted from the close vicinity of the compact object, through the winds of the accretion disk and of the stellar companion

To the right: Artist's impression of SS433
(no circumbinary disk included)
(Wikipedia's page on SS433)



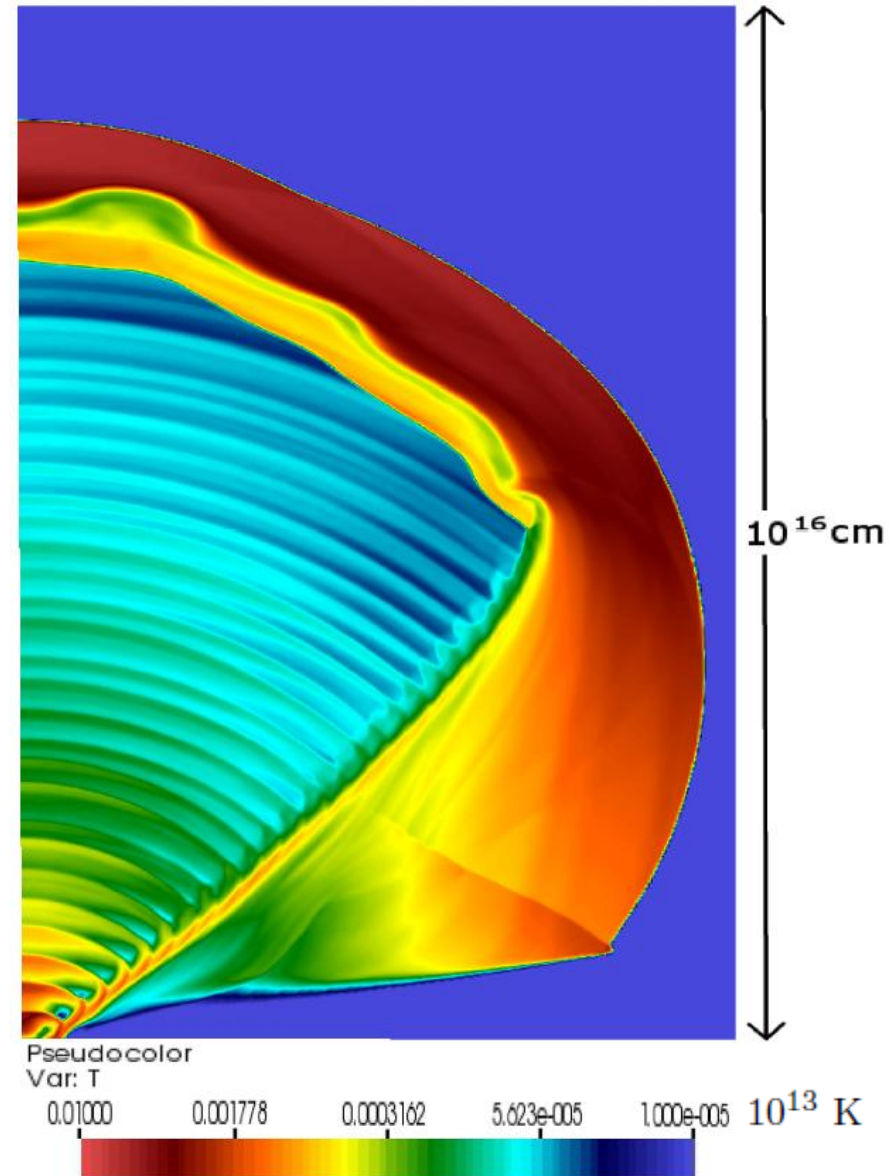
Model setup

- 3D Special Relativistic Hydrodynamics simulations
- PLUTO code (Mignone et al. 2007)
- Grid XYZ cartesian $250 \times 750 \times 250$ (homogeneous)
- jet origin at base of y axis, moving along y axis (axial symmetry assumed: y is jet axis)
- no jet precession
- PPM method (Colella & Woodward 1984)
- Jet crosses a $1/r^2$ stellar wind from binary, and also a simplified accretion disk wind
- Both stars share same computational cell
- Extended disk included



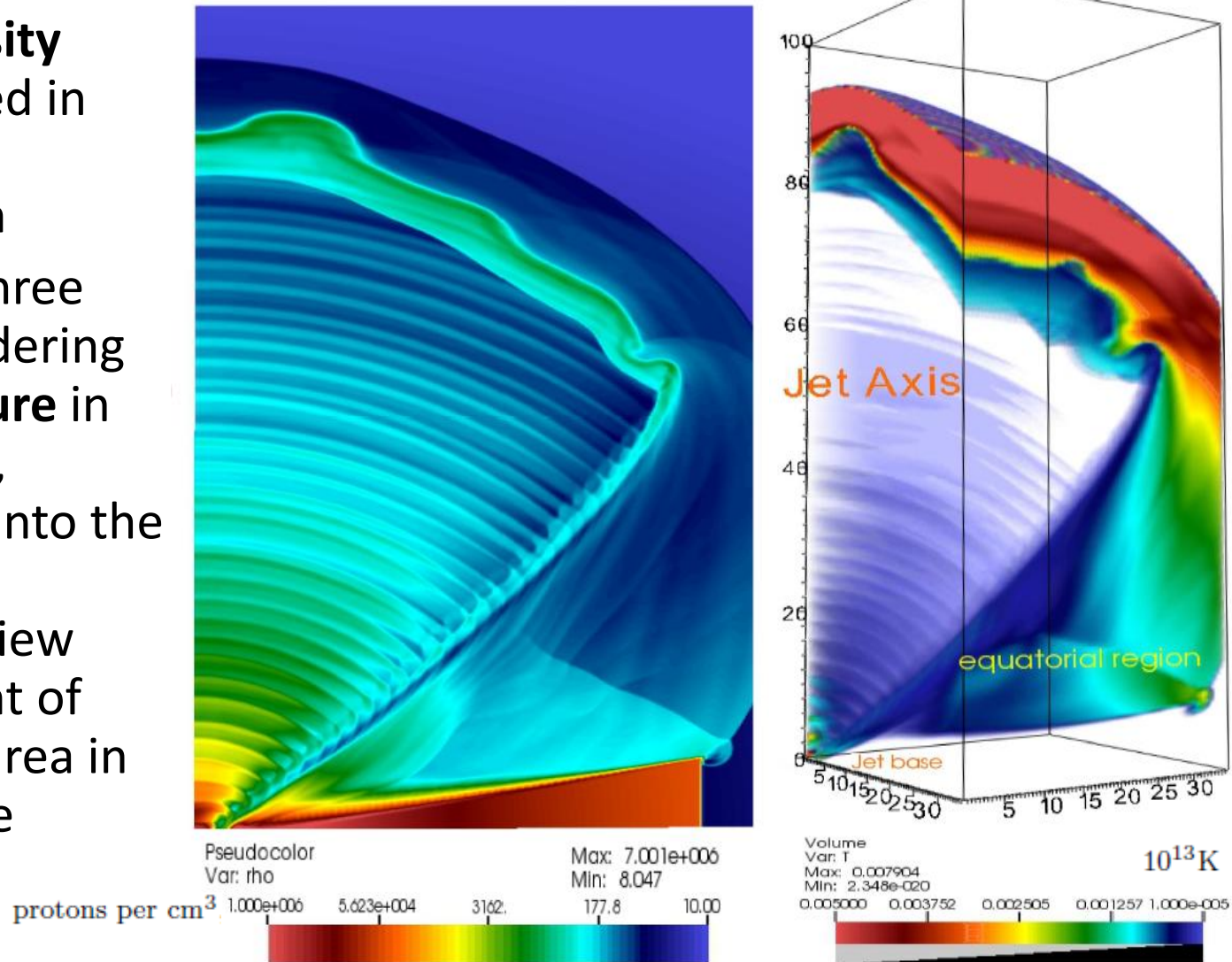
Results: Heavy jet

- Jet density 10^6 , initial ambient density 10^5 (protons/cm³)
- Equatorial region appears active, due to converging shocks:
- From outer expanding jet portion (partially retreating shock)
- And from inner jet sideshock
- Extended disk facilitates matter containment at equatorial region
- Right: A 2D slice from a 3D model grid is shown, at model time 400 hrs after the beginning of -pulsed-jet ejection.



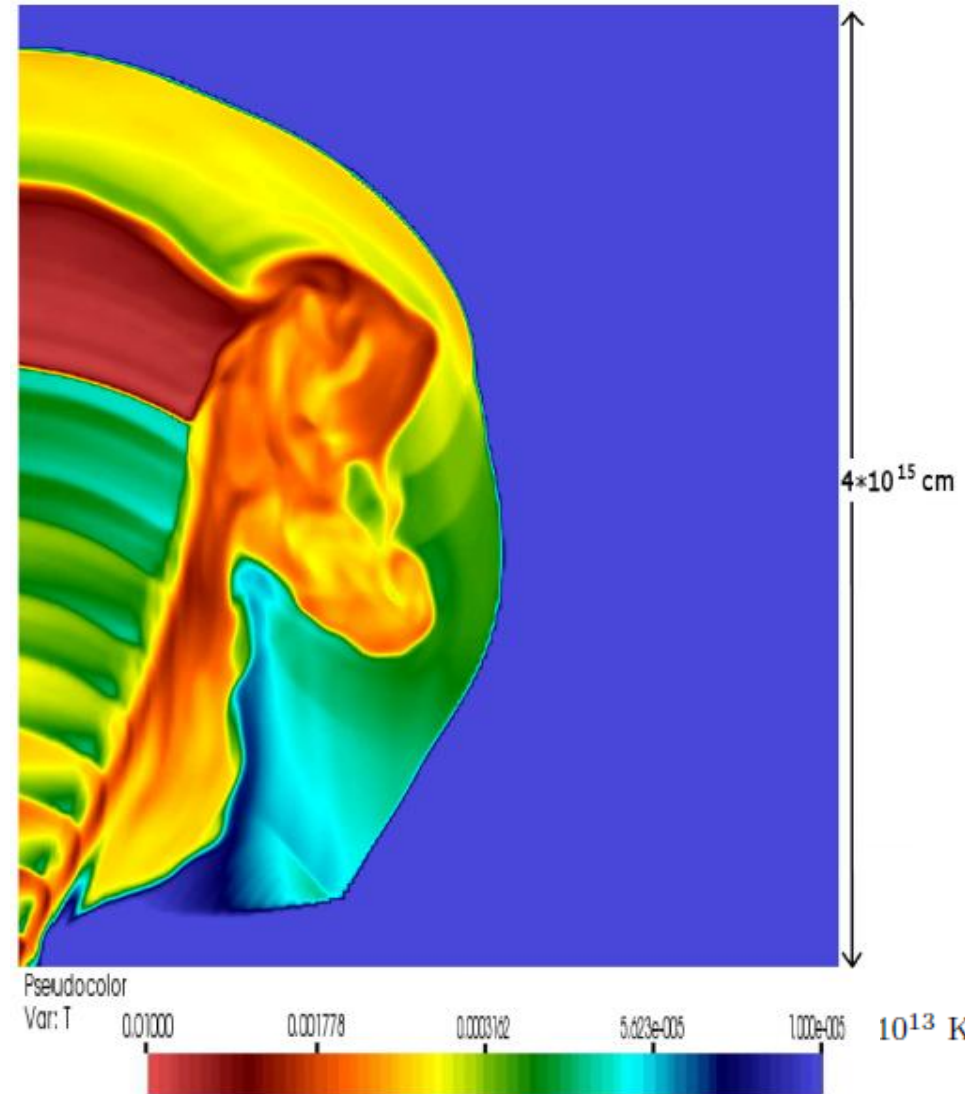
Results: Heavy jet (2)

- **Left Figure: Density** appears enhanced in active portion of equatorial region
- **Right Figure:** A three dimensional rendering of the **temperature** in the model space, roughly halfway into the simulation. The (hopefully!) 3D view reveals the extent of activity over an area in the vicinity of the extended disk



Results: Light jet

- Jet density 10^4 , initial ambient density 10^5 (protons/cm³)
- This time results are similar to the heavier jet case...
- but the equatorial region of interest appears closer to the jet
- Slice time mark: around half way into the model run
- Slower spatial expansion of active equatorial region
- Longer lived effects



Thermal imaging

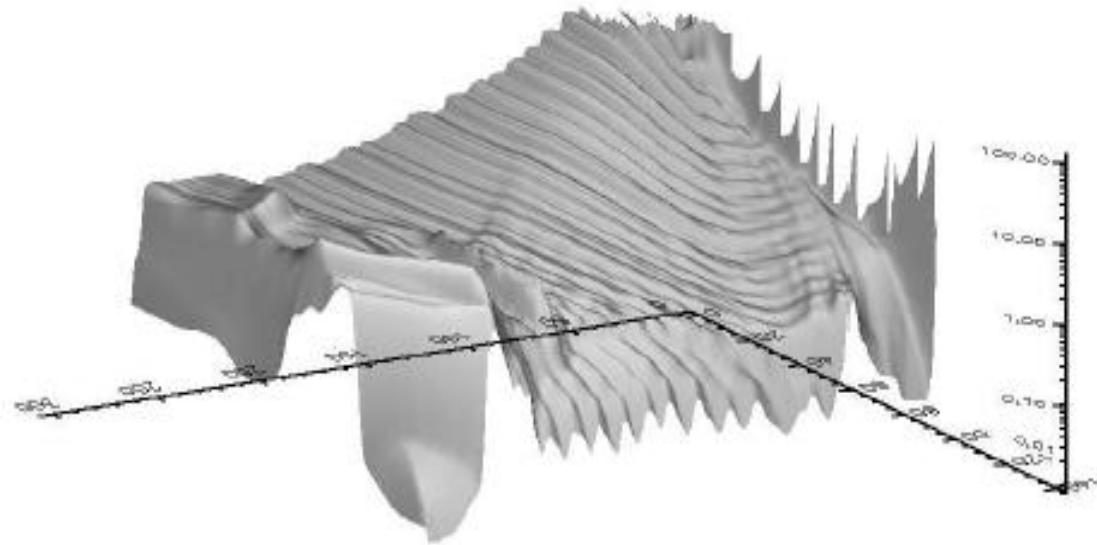


Figure 6. A synthetic view of the thermal radio emission (logarithmic plot) of the heavy jet system at 8 GHz, around model time 450. The value of the intensity has been calculated in units of $10^6 \text{ erg}/(\text{Hz} \times \text{sr})$ per 1 s time interval, i.e. erg per sr per Hz per s. The length units along the bottom plane axes are in radiative code cell lengths of 2.7×10^{13} cm. The jet base is at the top corner, the jet axis is along the top left side and the equatorial region appears slightly above the middle of the top right side. A ridge of locally increased emission there indicates the equatorial emission. A further increase of emission at the side of the jet is seen along the extended disk surface, along the top right side.

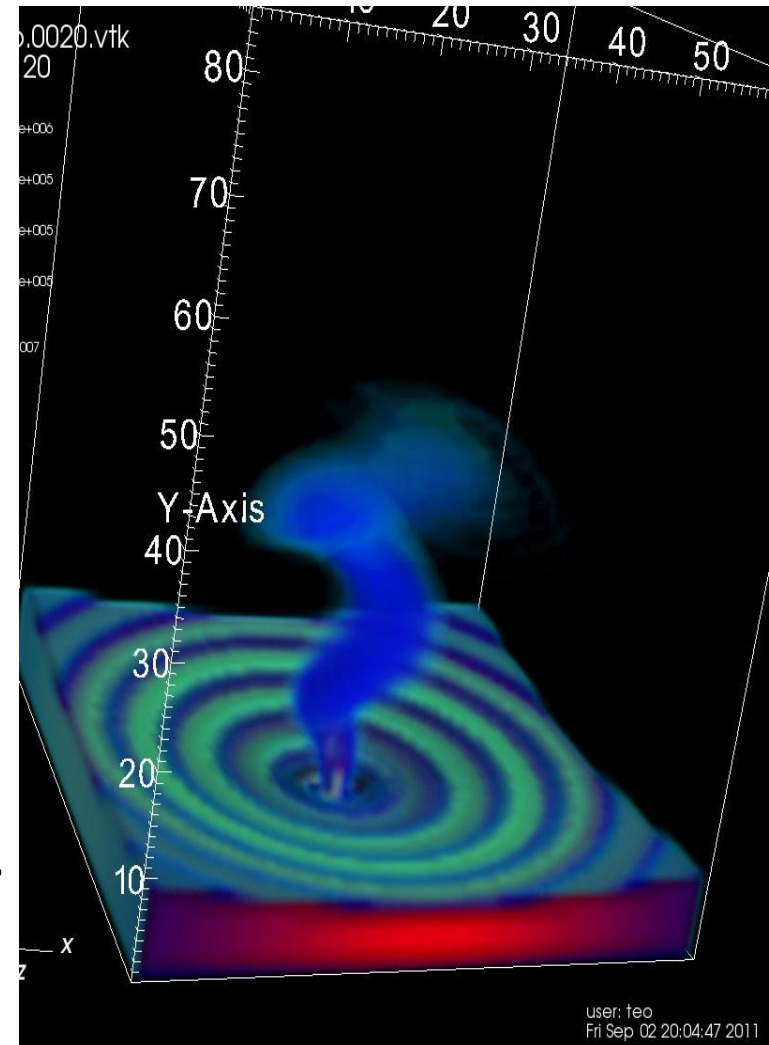
- The equation of radiative transfer is solved along...
- ...lines of sight (LOS) drawn through...
- ...3D domain of a snapshot of PLUTO's results
- Thermal radio emission coefficient calculated per grid cell, from hydro quantities (ρ , T) at that cell
- Self absorption included, but proves to be small in our case

Thermal imaging (2)

- The code to calculate the thermal emission and absorption crossed the hydrocode results' 3D domain in a zig-zag manner, always trying to stay as close as possible to a predefined (azimuth and elevation compared to the jet axis) direction. This defined a 1D array of a line of sight.
- Along that line, the equation of radiative transfer was then solved.
- Many such lines were drawn, each of them with a different initial point. The emission of each line of sight was assigned to a pixel of the final artificial image.

Conclusions

- Attempt to simulate the suggested mechanism of jet-wind-extended disk interaction
- Model setup is rather generic for a microquasar, as long as an adequate stellar wind is present
- Therefore results may concern more systems
- Recent update: A precessing jet shows enhanced equatorial activity where the jet comes closer to the equatorial region.
- (Right: Density plot of a model precessing jet).



Ongoing work

- Apart from modelling a precessing jet,
- special relativistic imaging (time travel effects taken into account when drawing the artificial map of the system)
- gamma ray and neutrino imaging (with and without self absorption, respectively), using approximate emission coefficients (Kelner et al. 2006) (at a much smaller spatial scale than for the radio simulations)

Acknowledgements

- TS's contribution to this project built on his work as a PhD student at Jodrell Bank Observatory, the University of Manchester, UK, under the supervision of R. Spencer and in collaboration with T. O'Brien.
- TS thanks Dr Sinatkas at the TEI of Kastoria, for assisting him to complete this project.

Bibliography

- Smponias, T. & Kosmas, T., Modelling the equatorial emission in a microquasar, MNRAS, 2, 412, 1320, 2011 (**See also references therein for a more complete bibliography on this presentation**)
- A. Mignone , G. Bodo , S. Massaglia , T. Matsakos , O. Tesileanu , C. Zanni , and A. Ferrari. PLUTO: A Numerical Code for Computational Astrophysics. The Astrophysical Journal Supplement Series, 170:228-242, 2007
- Kelner, S. R., Aharonian, F. A., Bugayov, V. V., Energy spectra of gamma rays, electrons, and neutrinos produced at proton-proton interactions in the very high energy regime. Phys. Rev. D, 74, 034018, 2006
- Colella, P.; Woodward, P. R. (April 1984). "[Piecewise parabolic method \(PPM\) for gas-dynamical simulations](#)". [J. Comput. Phys. \(Elsevier\)](#) **54** (1): 174–201